International Journal of Mathematical Archive-9(5), 2018, 191-202
Available online through www.ijma.info ISSN 2229 – 5046

# MAGNETOHYDRODYNAMIC TWO-PHASE DUSTY FLUID FLOW AND HEAT MODEL OVER RIGA PLATE WITH DEFORMING ISOTHERMAL SURFACES IN THE PRESENCE OF NONLINEAR THERMAL RADIATION

**MALLIKARJUNA H.B, JAYAPRAKASH M.C* AND RAGHAWENDRA MISHRA**

**Department of Mathematics.**
**Adichunchanagiri Institute of Technology. Chikkmagalore, Karnataka, INDIA.**

**Department of Information Technology,**
**Al Musanna College of Technology, Sultanate Of Oman.**

**Department of Mathematics,**
**Government Post Graduate College, Ranikhet, (Almora), INDIA.**

***(Received On: 02-01-18; Revised & Accepted On: 25-04-18)***

***ABSTRACT***

*The present work deals with the study of MHD viscous two-phase dusty flow and heat transfer over a Riga plate with permeable stretching body in the presence of non linear thermal radiation. The wall boundary is subjected to a linear deformation as well as to a quadratic surface temperature. Similarity transformations are utilized to reduce the governing partial differential equations into a set of nonlinear ordinary differential equations. The reduced equations were numerically solved using Runge-Kutta-Fehlberg fourth-fifth order method along with shooting technique. The impact of various pertinent parameters for the velocity and temperature fields are profiles are analyzed through graphs in detail. Also, friction factor and Nusselt numbers are discussed and presented through graphs.*

**Keywords:** *Two phase flow; Dusty fluid, Riga plate, Nonlinear thermal radiation, Runge-Kutta-Fehlberg fourth-fifth order method.*

## 1. INTRODUCTION

The analysis of the flow of fluids with gas–particle mixture or suspended particles has received notable attention due to its practical applications in various problems of atmospheric, engineering, and physiological fields. Typical examples occurring in nature are forest-fire smoke, dust storms and the dispersion of the solid pollutants in atmosphere. In addition, solid rocket exhaust nozzles, blast waves moving over the Earth's surface, fluidization in chemical reactors with gas–solid feeds, fluidized beds, petroleum industry, environmental pollutants, physiological flows, purification of crude oil and other technological fields are some of the practical problems where the dusty viscous flow found its applications. Other important applications involving dust particles in boundary layers include soil salvation by natural winds, lunar surface erosion by the exhaust of a landing vehicle and dust entrainment in a cloud formed during a nuclear explosion. Two-phase particulate suspension flows containing discrete particle phase and the continuous fluid phase have several engineering applications. Study of boundary layer flow and heat transfer in dusty fluid is very constructive in understanding of various industrial and engineering problems concerned with powder technology, nuclear reactor cooling, sedimentation, atmospheric fallout, rain erosion in guided missiles, fluidization, combustion, electrostatic precipitation of dust, acoustics batch settling, aerosol, waste water treatment and paint spraying and etc. Saffman [1] initially formulated the basic equations for the flow of dusty fluid, who derived the motion of gas equations carrying the dust particles. Vajravelu and Nayfeh [2] investigated the hydromagnetic flow of a dusty fluid over a porous stretching sheet. Since then many researchers have discussed and observed the phenomena of the mass and heat transfer of dusty fluid flow between parallel plate and over a stretching surface under different thermal conditions. Gireesha *et al.* [3] described the boundary layer flow and heat transfer analysis of dusty fluid past a stretching sheet in the presence of non-uniform heat source/sink. Manjunatha *et al.* [4] numerically investigated the steady two dimensional flow and heat transfer analysis of dusty fluid towards a stretching cylinder embedded in a porous media under the influence of non-uniform source/sink. Prasannakumara *et al*. [5] analyzed the effect of thermal radiation, nonuniform heat source/sink on the flow of two-dimensional incompressible viscous dusty fluid over a

***Corresponding Author: Jayaprakash M.C****

melting stretching surface. Turkyilmazoglu [6] studied the magnetohydrodynamic flow of a two-phase viscous dusty fluid and heat transfer over a shrinking bodies or permeable stretching. Recently, Gireesha *et al.* [7] numerically investigate the effect of thermal stratification on magnetohydrodynamic flow and heat transfer of dusty fluid towards a vertical stretching sheet immersed in a thermally stratified porous media in the presence of thermal radiation and uniform heat source.

The control device of Gailitis and Lielausis which is electromagnetic actuator which consists of a spanwise aligned array of alternating electrodes and permanent magnets, mounted on a plane surface (see Fig. 2). This set up referred as Riga plate can be applied to reduce the friction and pressure drag of submarines by preventing boundary layer separation. Gailitis and Lielausis [8] of the Physics institute in Riga, Latvia, initiated the device riga plate to generate a crossed electric and magnetic field which may manufacture a wall parallel Lorentz force so as to regulate the fluid flow. Pantokratoras and Magyari [9] studied basic aspect of electro-magnetohydrodynamic free-convection boundary layer flow of a see water like weekly conducting fluid over the horizontal Riga plate. Magyari and Pantokratoras [10] investigated the Blasius flow of an electrically conducting fluid over the Riga-plate. He showed that modified Hartmann number is positive for aiding flow and negative for opposing flow. Hayat *et al.* [11] presented a computational modelling to analyze the effect of heat generation/absorption on the boundary layer flow of a nano fluid induced by a variable thickened Riga plate with convective boundary condition. Ahmad *et al.* [12] obtained a analytical solution by perturbation method for small Brownian and thermophoresis diffusion parameters to study the mixed convection boundary layer flow of a nanofluid past a vertical Riga plate in the presence of strong suction. He also shown that skin friction can be controlled by taking an appropriate size and quality of the nanoparticles and adjusting the magnitude of flow Lorentz force due to Riga plate. Ayub *et al.* [13] examined the simultaneous effects of EMHD and slip on the flow of nanofluids over a horizontal Riga plate. The simultaneous effects of thermal radiation and EMHD on viscous nanofluid through a horizontal Riga plate have been analyzed by Bhatti *et al.* [14]. Entropy generation on viscous nanofluid with mixed convection boundary layer flow induced by a horizontal Riga plate has been examined by Abbas *et al.* [15]. In the presence of a strong magnetic field, Hayat *et al.* [16] explored the structure of convective heat transfer of electromagnetohydrodynamic squeezed flow past a Riga plate.

Role of radiation heat transfer is superficial in many engineering processes which occur at high temperature. A substantial number of experimental and theoretical studies have been carried out by numerous researchers on radiation effect [17-18]. In most of the above cited literature, linearized Rosseland approximation has been considered for radiation effect. This type of approximation involves the dimensionless parameters called Radiation parameter and Prandtl number which are sustainable if the temperature difference between the plate and ambient fluid is small. But, for the larger temperature difference nonlinearized Rosseland approximation is valid. Ramesh *et al.* [19] theoretically studied the steady stagnation point flow with heat transfer of nanofluid towards a stretching surface. Pal *et al.* [20] investigated the combined effects of thermal radiation and internal heat source/sink on the thin film flow and mass transfer towards a permeable stretching sheet in the presence of suction/injection and chemical reaction. Ramesh *et al* [21] numerically analyzed three-dimensional flow fills the porous space bounded by a bidirectional stretching sheet with non-linear thermal radiation and heat source/sink. Recently, Hayat *et al.*. [22] analyzed the nonlinear thermal radiation aspects in the two-dimentional mixed convection stagnation point flow of double diffusive convection in tangent hyperbolic nanofluid towards a permeable stretching surface.

To the author's Knowledge no studies have been reported yet on boundary layer flow of two -phase dusty fluid model over a stretching surface with Riga-plate in an electrically conducting fluid when mass flow transfer through the surface is permitted, in the presence of nonlinear thermal radiation. The governing equation are transformed into non linear ordinary differential equation by using similarity transformation and then solved numerically using Runge –Kutta-Fehlberg-45 order method with shooting technique. The behaviors of each of the nondimensional quantities are exposed graphically for all the fluid parameters. Also, friction factor and Nusselt numbers are discussed and presented through graphs.

## 2. FORMULATION

Consider a steady two dimensional motion of boundary layerflow over a permeable Riga plate with stretching isothermal sheet through a quiescent incompressible viscous electrically conducting dusty fluid. Refer to figure 1 and figure 2 for a simple sketch of the problem. The stretching/shrinking sheet coincides with the plane $y = 0$. It is assumed that the velocity of the sheet is linear, that is $u_w(x) = cx$, with $c > 0$ for a stretching sheet and $c < 0$ for a shrinking sheet. It is also assumed that the local temperature of the sheet is $T_w$, while that of the ambientfluid and dust particles is$T_\infty$. A uniform magnetic field $B_0$ is applied in the transverse direction $y > 0$ normal to the plate. The dust particles are assumed to be spherical in shape, uniform in size possessing constant number density.

Under these assumptions, along with the usual boundary layer approximations, the governing equations for the flow are,

$$\frac{\partial u}{\partial x} + \frac{\partial v}{\partial y} = 0, \tag{1}$$

$$u\frac{\partial u}{\partial x}+v\frac{\partial u}{\partial y}=v\frac{\partial^2 u}{\partial y^2}+\frac{KN}{\rho}\left(u_p-u\right)+\frac{\pi j_0 M_0}{8\rho}\exp\left(-\frac{\pi}{a}y\right), \tag{2}$$

$$\frac{\partial u_p}{\partial x}+\frac{\partial v_p}{\partial y}=0, \tag{3}$$

$$u_p\frac{\partial u_p}{\partial x}+v_p\frac{\partial u_p}{\partial y}=\frac{K}{m}\left(u-u_p\right), \tag{4}$$

$$\rho c_p\left(u\frac{\partial T}{\partial x}+v\frac{\partial T}{\partial y}\right)=k\frac{\partial^2 T}{\partial y^2}+\frac{\rho_p c_m}{\tau_T}\left(T_p-T\right)+\frac{\rho_p}{\tau_v}\left(u_p-u\right)^2-\frac{\partial q_r}{\partial y}, \tag{5}$$

$$\rho_p c_m\left(u_p\frac{\partial T_p}{\partial x}+v_p\frac{\partial T_p}{\partial y}\right)=\frac{\rho_p c_m}{\tau_T}\left(T_p-T\right), \tag{6}$$

with the fluid and dust particle boundary conditions

$$u=U_w(x)=cx, v=0, T=T_w(x)=T_\infty+bx^2 \text{ at } y=0,$$
$$u\to 0, u_p\to 0, v_p\to v,\ T\to T_\infty, T_p\to T_\infty \text{ as } y\to\infty. \tag{7}$$

In the above expressions, where here $(u,v)$ and $(u_p,v_p)$ are the velocity components of the fluid and dust particle phases along $x$ and $y$ directions respectively. $v,K,N,\rho$ are the kinematic viscosity of the fluid, Stokes resistance or drag coefficient, number of dust particle per unit volume, density of thefluid respectivel y. $j_0$ is the applied current density in the electrodes, $M_0$ is the magnetization of the permanent magnets mounted on the surface of the Riga plate, $a$ denotes the width of the magnets between the electrodes, $m$ is the mass of the dust particle. $T$ and $T_p$ is the temperature of the fluid and temperature of the dust particle respectively, $c_p$and $c_m$ are the specific heat of fluid and dust particles, $\tau_T$ is the thermal equilibrium time i.e., the time required by the dust cloud to adjust its temperature to the fluid, $\tau_v$ is the relaxation time of the of dust particle i.e., the time required by a dust particle to adjust its velocity relative to the fluid. Further, $b$ is a constant with $b>0$ for a heated plate $(T_w>T_\infty)$ and $b<0$ for a cooled surface $(T_w<T_\infty)$, respectively. It should be noted that the rest of the momentum equations regarding the fluid and dust particles, which are not cited in Equation (1), can be made use of evaluating the pressures acting upon thefluid and dust, which is a trivial task, so omitted here.

To underline the fundamental assumptions adopted for the current physical phenomenon, we use a constant drag force, to model the interaction between the viscousfluid and the particle phase, where $K$ is defined as $6\pi\rho v r$ for a free falling sphere with $r$ being the sphere radius. For suspensions of particles that tend to follow the fluid (convective and local acceleration neglected compared to the viscous term), to idealize the model, $K$ is presently taken as independent of the relative velocity betweenfluid and dust. However, assuming $K$ being independent of the vertical position implies that there is no influence of the vicinity of the sheet on the hydrodynamic forces acting on the spheres. Besides, close to the sheet, it is assumed that the spheres are subjected to a shear flow produced by the stretching/shrinking of the wall. This would lead to a drag experienced by the sphere not only due to its translational motion but also due to a certain shear flow, and to the induced rotational motion. Furthermore, no interaction between the spheres is allowed within the present approach.

Using Rosseland approximation for radiation, the nonlinear radiative heat flux $q_r$ is simplified as,

$$q_r=-\frac{4\sigma^*}{3k^*}\frac{\partial T^4}{\partial y}=-\frac{16\sigma^*}{3k^*}T_\infty{}^3\frac{\partial T}{\partial y}. \tag{8}$$

where $\sigma^*$ is the Stefan–Boltzmann constant and $k^*$ is the mean absorption coefficient. Here energy equation takes the form as follows

$$\rho c_p\left(u\frac{\partial T}{\partial x}+v\frac{\partial T}{\partial y}\right)=\frac{\partial}{\partial y}\left[\left(k+\frac{16\sigma^* T_\infty{}^3}{3k^*}\right)\frac{\partial T}{\partial y}\right]+\frac{\rho_p c_m}{\tau_T}\left(T_p-T\right)+\frac{\rho_p}{\tau_v}\left(u_p-u\right)^2. \tag{9}$$

The mathematical analysis of the current physical problem is simplified by introducing the subsequent similarity transformations based on the dimensionless boundary layer coordinate $\eta$,

$$u=cxf'(\eta),\ v=-\sqrt{cv}\,f(\eta),\ \eta=\sqrt{\frac{c}{v}}y,$$
$$u_p=cxF'(\eta),\ v_p=-\sqrt{cv}F(\eta),\quad \theta(\eta)=\frac{T-T_\infty}{T_w-T_\infty},\ \theta_p(\eta)=\frac{T_p-T_\infty}{T_w-T_\infty}, T_w-T_\infty>0 \tag{10}$$

where, $T_w$ and $T_\infty$ denote the temperature at the wall and at large distance from the wall, respectively. With $T=T_\infty(1+(\theta_w-1)\theta')$ and $\theta_w=\frac{T_w}{T_\infty}$ is the temperature ratio parameter.

The governing equations of motion for the two-phase fluid flow and heat transfer equation (2), (4), (6) and (9) are then reduced to

$$f'''+ff''-(f')^2+\ l\beta[F'-f']+\mathrm{Q}\exp(-\mathrm{A}\eta)=0, \tag{11}$$
$$F'^2-FF''+\beta[F'-f']=0, \tag{12}$$
$$\left((1+Rd(1+(\theta_w-1)\theta)^3)\theta'\right)'+\Pr[f\theta'-2f'\theta]+Prl\gamma\beta_T\left(\theta_p-\ \theta\right)+l\beta\Pr Ec(F'-f')^2=0 \tag{13}$$
$$2F'\theta_p-F\theta'_p+\beta_T\left(\theta_p-\theta\right)=0. \tag{14}$$

*© 2018, IJMA. All Rights Reserved* 

The corresponding boundary conditions will takes the following form,

$$f(0) = 0, f'(0) = 1, \theta(0) = 1$$

$$f'(5) = 0, F'(5) = 0, F(5) = f(5), \theta(5) = 0, \theta_p(5) = 0 \tag{15}$$

where $l = \frac{\rho_p}{\rho}$ is the mass concentration of dust particles (or particle loading parameter) with $\rho_p = Nm$, standing for the density of the particle phase, $\beta = \frac{1}{c\tau_v}$ is thefluid particle interaction parameter for velocity, $Rd = \frac{16\sigma^* T_\infty^3}{3kk^*}$ is the radiation parameter, $Q = \frac{\pi j_0 M_0}{8\rho c^2 x}$ is the modified Hartman number, $A = \frac{\pi/a}{c/\nu}$ is the dimensionless parameter, $Pr = \frac{\nu \rho c_p}{k}$ is the Prandtl number, $\gamma = \frac{c_m}{c_p}$ is the specific heat parameter, $\beta_T = \frac{1}{c\tau_T}$ is the fluid -interaction parameter for temperature, and $Ec = \frac{c^2}{bc_p}$ is the Eckert number.

The physical quantities of interest are the skin friction coefficient $C_f$ and the local Nusselt Number $Nu$ which are defined as

$$C_{fx} = \frac{\tau_w}{\rho U_w^2}, \qquad Nu = \frac{xq_w}{k(T_w - T_\infty)} \tag{16}$$

where the surface shear stress $\tau_w$ and the surface heat flux $q_w$ are given by

$$\tau_w = -\mu\left(\frac{\partial u}{\partial y}\right)_{y=0}, \qquad q_w = -k\left(\frac{\partial T}{\partial y}\right)_{y=0} + (q_r)_w. \tag{17}$$

Using the nondimensional variables, we obtain

$$C_{fx} Re_x^{\frac{1}{2}} = -f''(0), \qquad Nu Re_x^{-\frac{1}{2}} = -(1 + Rd\theta_w^3)\theta'(0). \tag{18}$$

## 3. NUMERICAL PROCEDURE

Equations (11)–(14) are highly non-linear ordinary differential equations. To solve these equations we adopted symbolic algebra software Maple and it is very efficient in using the well known Runge Kutta Fehlberg fourth–fifth order method (RKF45 Method) to obtain the numerical solutions. The coupled ordinary Eqs. (11) – (15) are solved by RKF45 method using Maple along with shooting technique.

## 4. RESULT AND DISCUSSION

Numerical computation is carried out to find the velocity and temperature profiles and are obtained by solving equations (11-14) when subjected to the boundary conditions (15) by assigning numerical values to the parameter encounter in the problem. The velocity filed and the temperature profile for both fluid and dust phases are plotted to investigate the influence of various flow controlling parameters such as mass concentration parameter $(l)$, fluid particle interaction parameter for velocity $\beta$, radiation parameter$(Rd)$, modified Hartman number $(Q)$, dimensionless parameter $(A)$, Prandtl number $(Pr)$, fluid interaction parameter for temperature $(\beta_T)$ and Eckert number $(Ec)$.

Impact of dimensionless parameter $A$ on velocity distribution is illustrated in Figure 3. It is analyzed that the velocity profile and associated boundary layer thickness decrease for higher values of $A$.

Figure 4 and 5 shows the behavior of mofied Hartman number $Q$ on the velocity and temperature distribution. It is observed that, the velocity profile increases and temperature profile decreases for increasing the values of $Q$. Further momentum boundary layer thickness also enhances. Due to fact that the greater influence of the modified Hartmann number $Q$, a considerable increase is observed in the fluid velocity.

The fluid and dust phase velocity distribution for fluid particle interaction parameter of velocity $(\beta)$ is shown in Figure 6. It is observed that an increase in fluid -particle interaction parameter, the thickness of momentum boundary layer decreases for fluid phase and this phenomena is opposite for the dust phase and which is as shown in Figure 6. From these figures observed that, the fluid phase velocity decreases and dust phase velocity increases for increasing the values of $\beta$. Effect of fluid particle interaction parameter of temperature $\beta_\tau$ on fluid and dust phase temperature profiles are shown in figure 7. It can be seen that fluid phase temperature decreases and dust phase temperature increases with increase in $\beta_T$.

Figure 8 shows the temperature profiles for the selected values of Eckert number $(Ec)$. It can be seen that the effect of increasing values of $Ec$ enhances the temperature at a point which is true for both the phases. This may happen due to the fact that heat energy is stored in the liquid due to frictional heating and this is true in fluid phase as well as dust phase.

Figure 9 represents the variation of temperature distributions for different values of Prandtl number $Pr$. It can be observed that the fluid phase and dust phase temperature decreases with increase of $Pr$. This is because the momentum boundary layer is thicker than the thermal boundary layer and consequently the temperature gradient decreases with the increase in Prandtl number.

Figure 10 illustrates the effects of the radiation parameter $(Rd)$ on the fluid phase and dust phase temperature, and from the graph it seen that as radiation parameter increases both the phases of temperature profile increases. This is due to the fact that an increase in radiation parameter provides more heat tofluid that causes an enhancement in the temperature and thermal boundary layer thickness.

Figure 11 illustrates the influence of temperature ratio parameter $(\theta_w)$ on temperature profile for both the phases. We noticed that the increase in temperature ratio parameter increases the thermal state of the fluid, resulting in to increase temperature profiles for fluid phase and dust phase. Physically, the fluid temperature is much higher than the ambient temperature for increasing values of $(\theta_w)$, which increases the thermal state of the fluid.

Figures 12 depicts the effect of mass concentration parameter $(l)$ on the velociy profile. In this figure, it is observed an increase in mass concentration of the particles decreases the momentum boundary layer for both the phases. It is noted from all the graphs that thefluid phase is parallel to that of dust phase and also the fluid phase is hi gher than the dust phase.

Figure 13 and depicts the effect of modified Hartman number $(Q)$,mass concentration parameter $(l)$ and modified Hartman number, fluid particle interaction parameter of velocity $(\beta)$ on skin friction coefficient respectively. Here we can notice that skin friction coefficient decreases with increase of these parameters respectively. It can also be concluded that skin friction coefficient is a increasing function modified Hartman number, mass concentration parameter and fluid particle interaction parameter of velocity.

Figure 15 and 16 depicts the effect of Radiation parameter, Temperature ratio parameter and Radiation parameter, Prandtl number on Nusselt number respectively. From figure 15 we can observed that, Nusselt number increases with increase of these parameters respectively. But opposite trend is observed in figure 15. It can also be concluded that Nusselt number is a increasing function of Radiation parameter, Temperature ratio parameter and also Prandtl number.

## 5. CONCLUSION

This paper addresses the transfer of momentum and energy of a MHD flow of a two-phase quiescent incompressible viscous electrically conducting dusty fluid over a Riga plate with permeable stretching body. The governing equations associated with the momentum and thermal fields are presented under the steady conditions. After applying the proper similarity transformations, a set of nonlinear ordinary differential equations is obtained by using similarity transformation, representing the flow of fluid and dust phases as well as temperature field of fluid and dust phases. After the nonlinear differential equation are solved numerically by using Runge-Kutta-Fehlberg-45 order method along with Shooting technique. The effects of various parameters on the flow and heat transfer are observed from the graphs, and are summarized as follows:

- Fluid phase velocity is always greater than that of the particle phase. And also fluid phase temperature is higher than the dust phase temperature.
- The effect of transverse modified Hartman number is to suppress the temperature field, which in turn causes the enhancement of the velocity field.
- Temperature profile increases for Eckert number, radiation parameter, temperature ratio parameter, and decreases for Prandtl number and mass concentration particle parameter.
- Increase of $\beta$ will decrease fluid phase velocity and increases dust phase velocity.
- Increase of $\beta_T$ will decrease fluid phase and increases dust phase of temperature profile.
- Skin friction coefficient is a increasing function modfied Hartman number , mass concentration parameter and fluid particle interaction parameter of velocity.
- Nusselt number is a increasing function of Radiation parameter, Temperature ratio parameter and also Prandtl number.

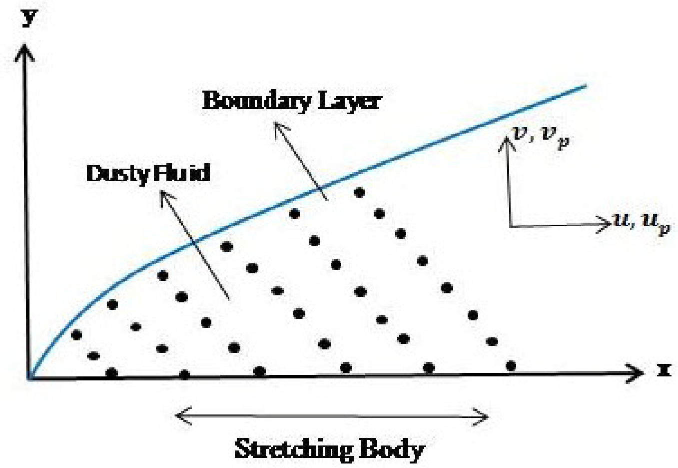


**Figure-1:** Schematic representation of the flow diagram.

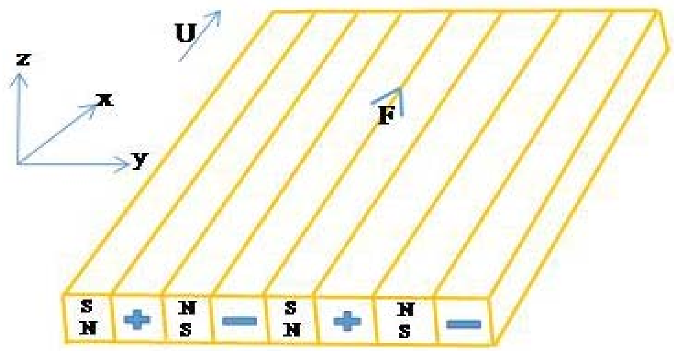


**Figure-2:** Riga plate.

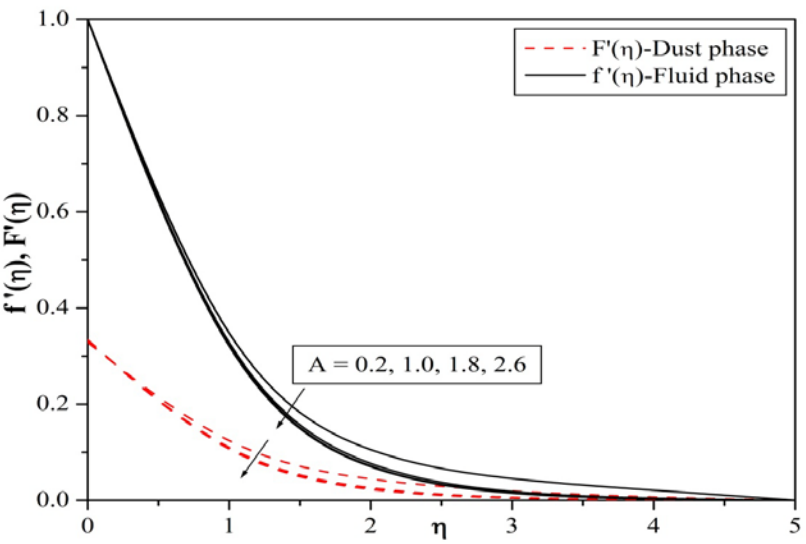


$Ec = 0.1, \Pr = 3.0, Q = 0.1, Rd = 1.0, \theta_w = 1.2, \beta = \beta_T = 0.5, l = 1.0$

**Figure-3:** Velocity profile for various values of dimensionless parameter $A$.

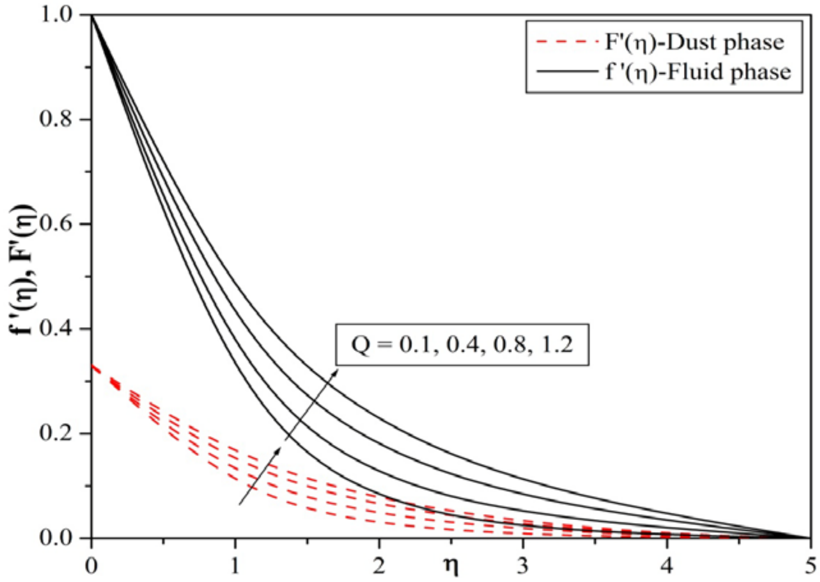


$A = 0.6, Ec = 0.1, \Pr = 3.0, Rd = 1.0, \theta_w = 1.2, \beta = \beta_T = 0.5, l = 1.0$

**Figure-4:** Velocity profile for various values of modified Hartman number Q.

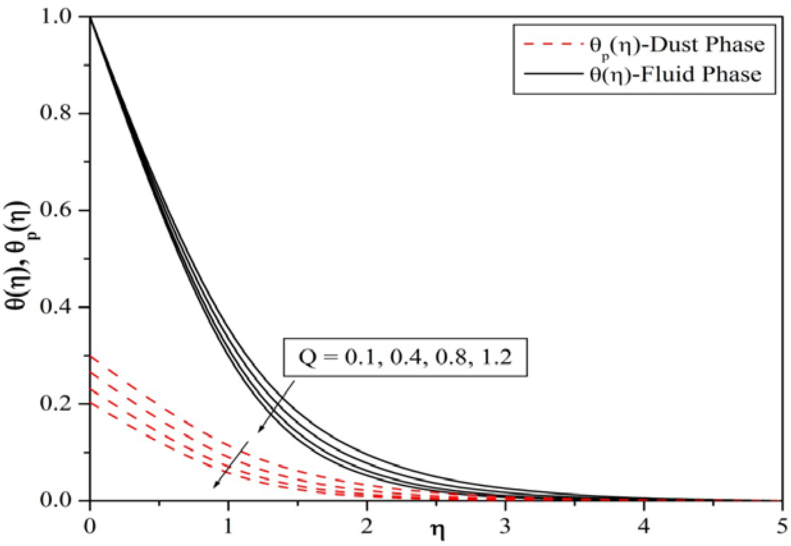


$A = 0.6, Ec = 0.1, \Pr = 3.0, Rd = 1.0, \theta_w = 1.2, \beta = \beta_T = 0.5, l = 1.0$

**Figure-5:** Temperature profile for various values of modified Hartman number $Q$.

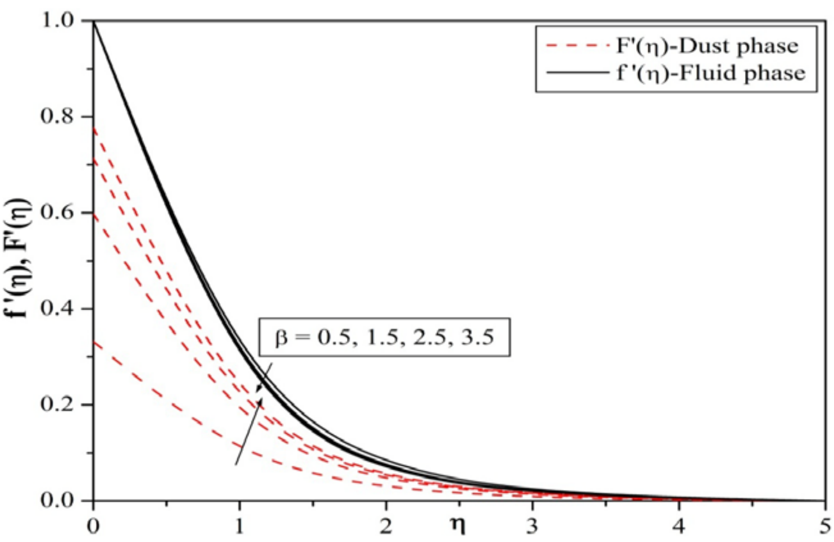


$A = 0.6, Ec = 0.1, \Pr = 3.0, Q = 0.1, Rd = 1.0, \theta_w = 1.2, \beta_T = 0.5, l = 1.0$

**Figure-6:** Velocity profile for various values of velocity fluid particle interaction parameter $\beta$.

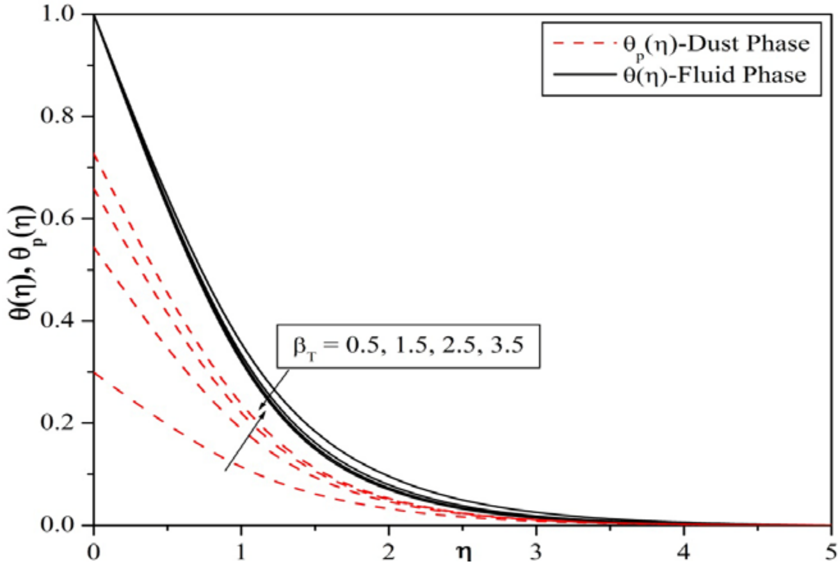


$A = 0.6, Ec = 0.1, \Pr = 3.0\,, Q = 0.1, Rd = 1.0, \theta_w = 1.2, \beta = 0.5, l = 1.0$

**Figure-7:** Temperature profile for various values of temperature fluid particle interaction parameter $\beta_T$.

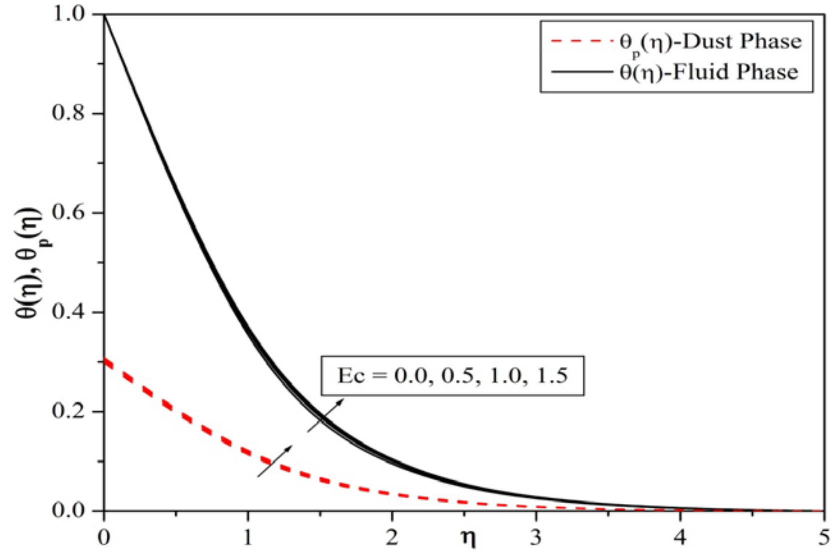


$A = 0.6, \Pr = 3.0\,, Q = 0.1, Rd = 1.0, \theta_w = 1.2, \beta = \beta_T = 0.5, l = 1.0$

**Figure-8:** Temperature profile for various values of Eckert number $Ec$.

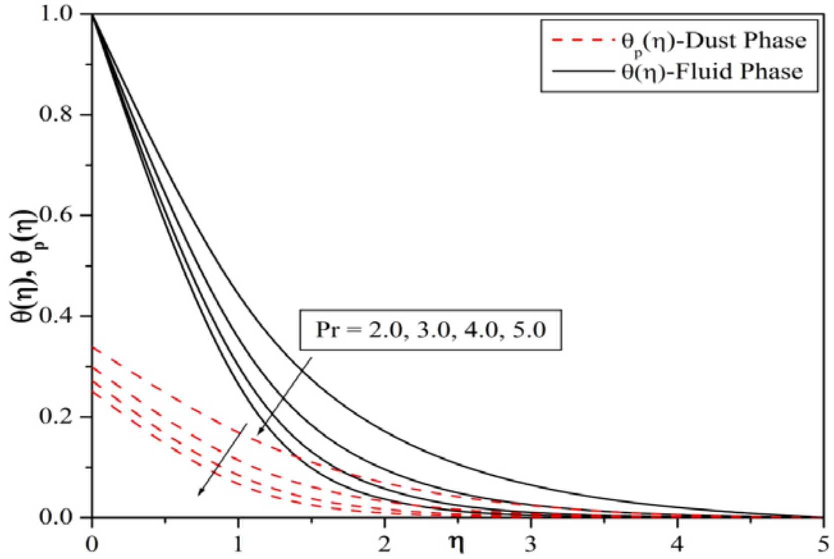


$A = 0.6, Ec = 0.1, Q = 0.1, Rd = 1.0, \theta_w = 1.2, \beta = \beta_T = 0.5, l = 1.0$

**Figure-9:** Temperature profile for various values of Prandtl number $Pr$.

*© 2018, IJMA. All Rights Reserved* 

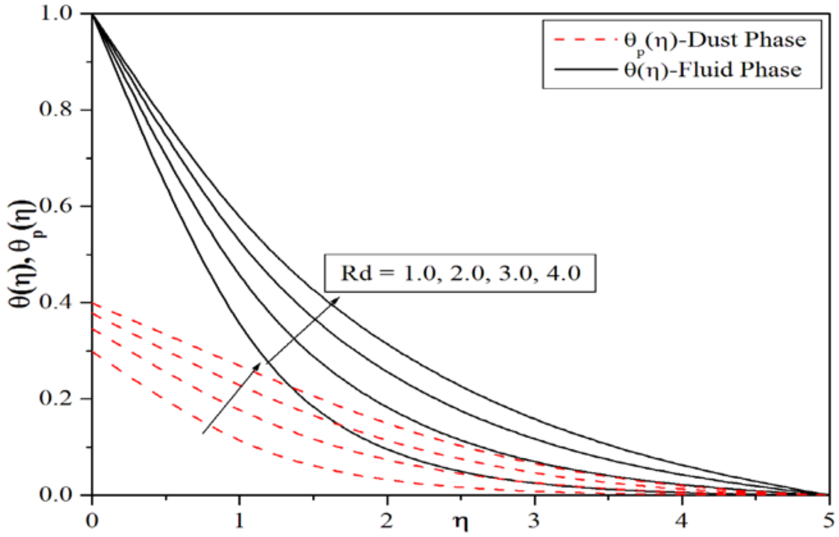


$A = 0.6, Ec = 0.1, Q = 0.1, \Pr = 3.0, \theta_w = 1.2, \beta = \beta_T = 0.5, l = 1.0$

**Figure-10:** Temperature profile for various values of radiation parameter $Rd$.

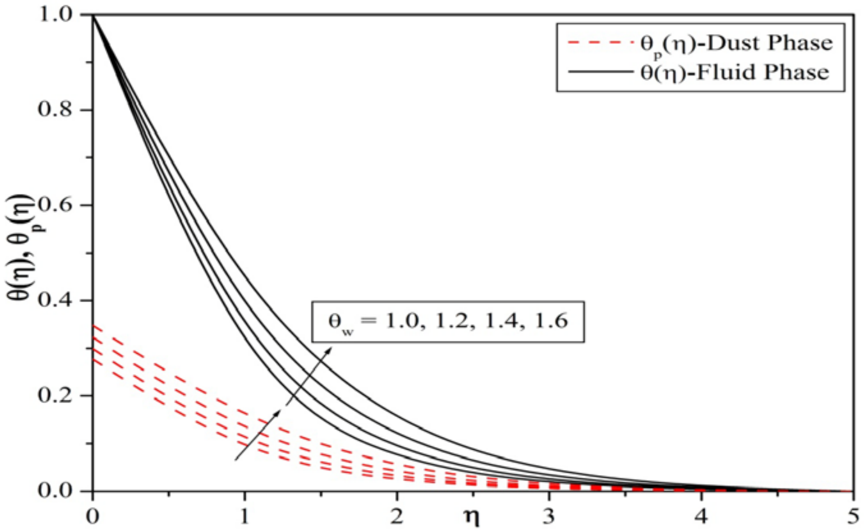


$A = 0.6, Ec = 0.1, Q = 0.1, \Pr = 3.0, Rd = 1.0, \beta = \beta_T = 0.5, l = 1.0$

**Figure-11:** Temperature profile for various values of temperature ratio parameter $\theta_w$.

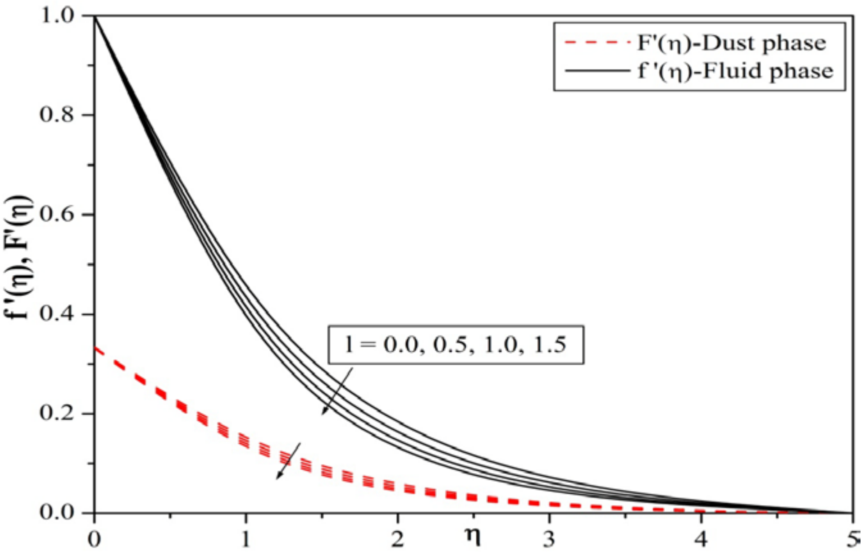


$A = 0.6, Ec = 0.1, \Pr = 3.0, Q = 0.1, Rd = 1.0, \theta_w = 1.2, \beta = \beta_T = 0.5, l = 1.0$

**Figure-12:** Velocity profile for various values of mass concentration particle parameter $(l)$.

© 2018, IJMA. All Rights Reserved

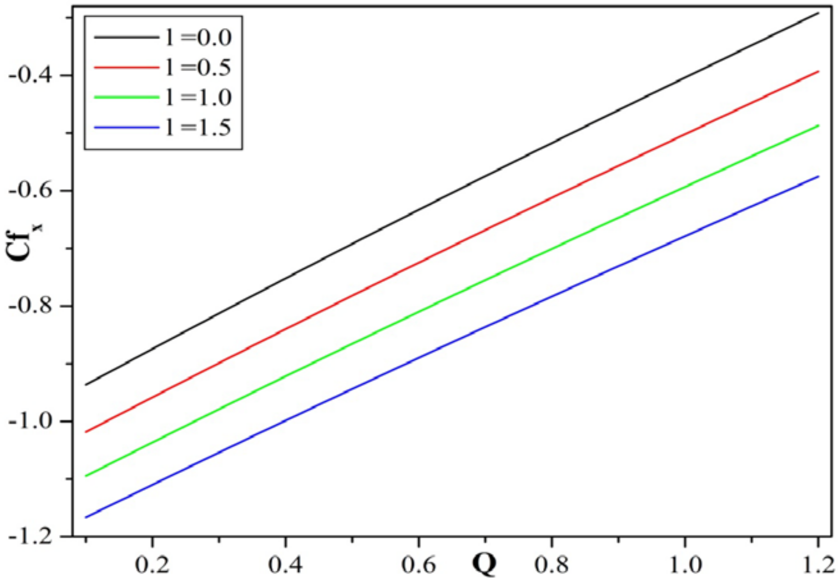


**Figure-13:** Effect of skinfriction for various values of $Q$ with $l$.

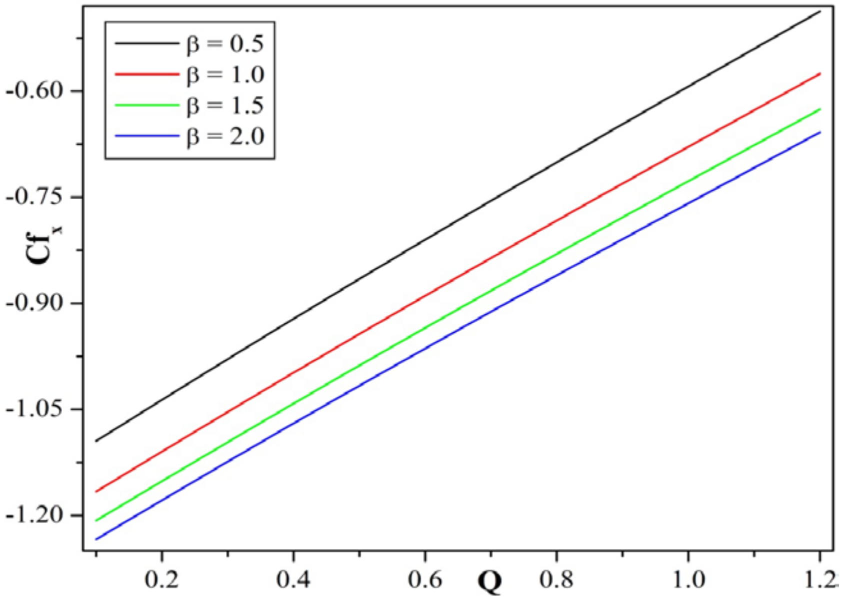


**Figure-14:** Effect of skinfriction for various values of $Q$ with $\beta$.

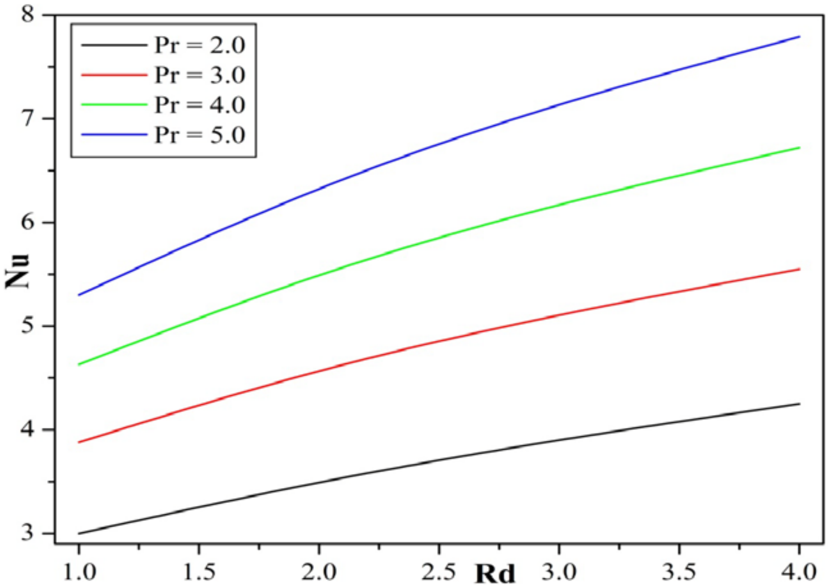


**Figure-15:** Effect of Nusselt number for various values of $Rd$ with $Pr$.

© 2018, IJMA. All Rights Reserved

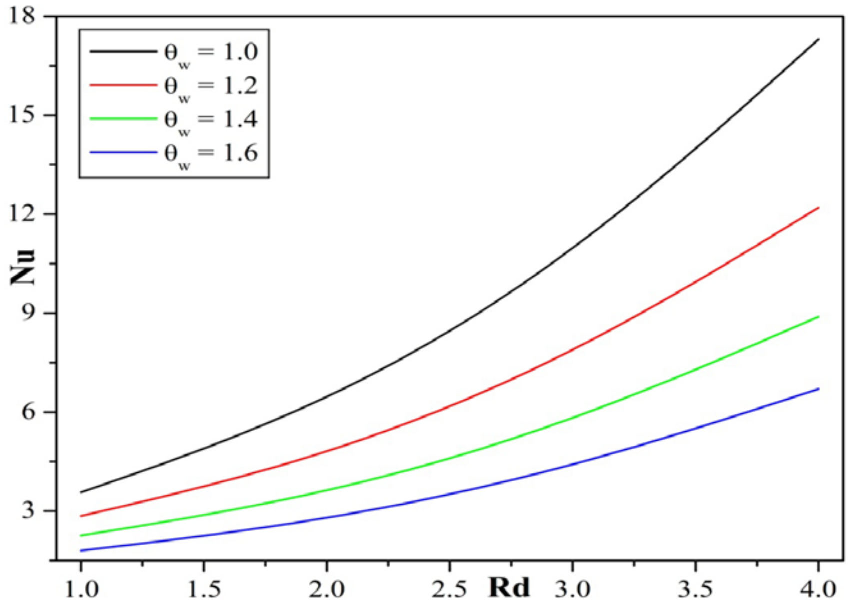


**Figure-16:** Effect of Nusselt number for various values of $Rd$ with $\theta_w$.

## REFERENCES


1. Saffman, P.G. On the stability of laminar flow of a dusty gas. *Journal of Fluid Mechanics*, 13, 120–128 (1962)
2. K.Vajravelu and J.Nayfeh, Hydromagnetic Flow of a Dusty Fluid over a Stretching Sheet, Int. J. of Nonlinear Mechanics, 27, pp. 937-945, 1992.
3. Gireesha, B. J., Ramesh, G. K., Abel, M. S., and Bagewadi, C. S., Boundary layer flow and heat transfer of a dusty fluid flow over a stretching sheet with non-uniform heat source/sink. *International Journal of Multiphase Flow*, 37, 977–982 (2011).
4. Manjunatha, P. T., Gireesha, B. J.,and Prasannakumara, B. C., Thermal analysis of conducting dusty fluid flow in a porous medium over a stretching cylinder in the presence of non-uniform source/sink. International Journal of Mechanical, 9(13), (2014) DOI: 10.1186/s40712-014-0013-8.
5. Prasannakumara, B. C., Gireesha, B. J.,and Manjunatha, P. T., Melting Phenomenon in MHD Stagnation Point Flow of Dusty Fluid over a Stretching Sheet in the Presence of Thermal Radiation and Non-Uniform Heat Source/Sink. *International Journal for Computational Methods in Engineering Science and Mechanics*, 16(5) (2015), http://dx.doi.org/10.1080/15502287.2015.1047056.
6. Turkyilmazoglu, M., Magnetohydrodynamic two-phase dusty fluid flow and heat model over deforming isothermal surfaces. *PHYSICS OF FLUIDS*, 29, 013302 (2017).
7. Gireesha, B. J., Venkatesh, P., Shashikumar, N. S., and Prasannakumara, B. C., Boundary layer flow of dusty fluid over a permeable radiating stretching surface embedded in a thermally stratified porous medium in the presence of uniform heat source. *Nonlinear Engineering*, (2017) DOI10.1515/nleng-2016-0058.
8. Gailitis, A., and Lielausis, O., On a possibility to reduce the hydrodynamic resistance of plate in an electrolyte. *Appl.Magnetohydrodyn*, 12, 143-146 (1961).
9. Pantokratoras, A., and Magyari, E, EMHD free-convection boundary-layer flow from a Riga-plate. *J.Eng. Math*., 64, 303–315 (2009).
10. Magyari, E., and Pantokratoras, A., Aiding and opposing mixed convection flows over the Riga-plate. *Commun Nonlinear Sci Numer Simulat*, 16, 3158–3167 (2011).
11. Hayat, T., Abbas, T., Ayuba, M., Farooq, M., and Alsaedi, A., Flow of nanofluid due to convectively heated Riga plate with variable thickness. *Journal of Molecular Liquids*, 222, 854–862 (2016)
12. Ahmad, A., Asghar, S., and Afzal, S., Flow of nanofluid pasta Riga plate. *Journal of Magnetism and Magnetic Materials*, 402, 44-48 (2016).
13. Ayub, M., Abbas, T., and Bhatti, M.M., Inspiration of slip effects on electromagnetohydrodynamics (EMHD) nanofluid flow through a horizontal Riga plate. *Eur. Phys. J. Plus*, 131(193), (2016) DOI 10.1140/epjp/i2016-16193-4.
14. Bhatti, M.M., Abbas, T., and Rashidi, M.M., Effects of thermal radiation and electromagnetohydrodynamic on viscous nanofluid through a Riga plate. *Multidiscipline Modeling in Materials and Structures*, 12(4), 605 – 618 (2016).
15. Abbas, T., Ayub, M., Bhatti, M.M., Rashidi, M.M., and El-Sayed Ali, M., Entropy Generation on Nanofluid Flow through a Horizontal Riga Plate. *Entropy*, 18(6), (2016) 223; doi: 10.3390/e18060223.
16. Hayat, T., Khan, M., Imtiaz, M., and Alsaedi, A., Squeezing flow past a Riga plate with chemical reaction andconvective conditions. *Journal of Molecular Liquids*, 225, 569–576 (2017).


© 2018, IJMA. All Rights Reserved

17. M. Gnaneswara Reddy, M.V.V.N.L. Sudha Rani and B.C.Prasannakumara., Non-Linear Radiation and Chemical Reaction Impacts on Hydromagnetic Particle Suspension Flow in Non-Newtonian Fluids, International Journal of Chemical Reactor Engineering, (2018), DOI: https://doi.org/10.1515/ijcre-2018-0001.
18. BC Prasannakumara, BJ Gireesha, RSR Gorla, MR Krishnamurthy, Effects of chemical reaction and nonlinear thermal radiation on Williamson nanofluid slip flow over a stretching sheet embedded in a porous medium. *Journal of Aerospace Engineering 29 (5), 04016019* (2016).
19. Ramesh, G. K, B. C. Prasanna Kumara, Gireesha, B. J, Rama Subba Reddy Gorla, MHD Stagnation Point Flow of Nanofluid Towards a Stretching Surface with Variable Thickness and Thermal Radiation. *Journal of Nanofluids, 4(2), 247-253(7)* (2015).
20. Pal, D., Saha, P., and Vajravelu, K., Combined Effects of Nonlinear Thermal Radiation and Internal Heat Generation/Absorption on Heat and Mass Transfer in a Thin Liquid Film on a Permeable Unsteady Stretching Surface with Convective Boundary Condition. *International Journal of Applied and Computational Mathematics*, 1–19 (2016) DOI: 10.1007/s40819-016-0242-z.
21. GK Ramesh, BC Prasannakumara, BJ Gireesha, SA Shehzad, FM Abbasi, Three dimensional flow of Maxwell fluid with suspended nanoparticles past a bidirectional porous stretching surface with thermal radiation. Thermal Science and Engineering Progress,,16-14 (2017).
22. Hayat, T., Qayyum, S., Alsaedi, A., and Shehzad, S.A., Nonlinear thermal radiation aspects in stagnation point flow of tangent hyperbolic nanofluid with double diffusive convection. *Journal of Molecular Liquids*, 223, 969–978 (2016).

**Source of support: Nil, Conflict of interest: None Declared.**

***[Copy right © 2018. This is an Open Access article distributed under the terms of the International Journal of Mathematical Archive (IJMA), which permits unrestricted use, distribution, and reproduction in any medium, provided the original work is properly cited.]***